STRUCTURAL
CHEMISTRY

Volume 74 (2018)

Supporting information for article:

Making an order: the concerted alignment of [*M*OF5]$^{2-}$ (*M* = Nb and Ta) dipolar anions in one-dimensional coordination chains sustained by tris(3,4,5-trimethyl-1*H*-pyrazole)copper(II)

Anastasiya V. Sharko, Oliver Erhart, Harald Krautscheid and Kostiantyn V. Domasevitch

Instrumentation

IR-spectra (400-4000 cm^{-1}) were measured with a Perkin Elmer FTIR spectrometer (KBr pellets). The room temperature (rt) powder X-ray diffraction (PXRD) patterns were measured using a Stoe STADIP (Cu-$K_{\alpha 1}$, using a 'Mythen' detector). Regarding peak positions, there is a very good coincidence between the experimental PXRD patterns of the obtained crystalline phases and the simulated patterns based on the single crystal structure (Mercury 3.3.1. software, CCDC). The temperature dependent X-ray measurements were recorded on a Stoe STADIP with a high temperature attachment and an image plate detector system. Simultaneous thermogravimetric/differential thermal analysis/mass spectrometry (TG/DTA-MS) studies were carried out on a Netzsch F1 Jupiter device connected to an Aeolos mass spectrometer. Samples were heated at a rate of 10 K min^{-1}.

Synthesis of the ligand:

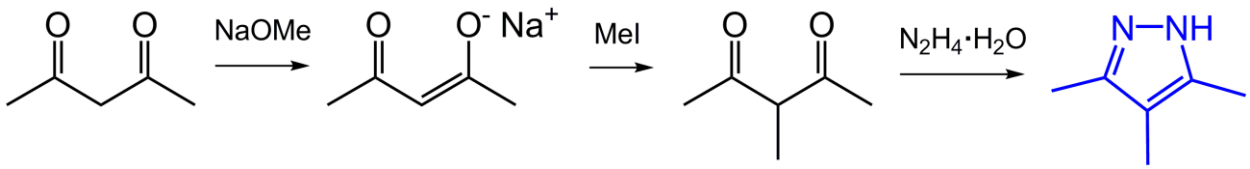

Chambers, D., Denny, W. A., Buckleton, J. S. & Clark, G. R. (1985). *J. Org. Chem*. **50**, 4736-4738.

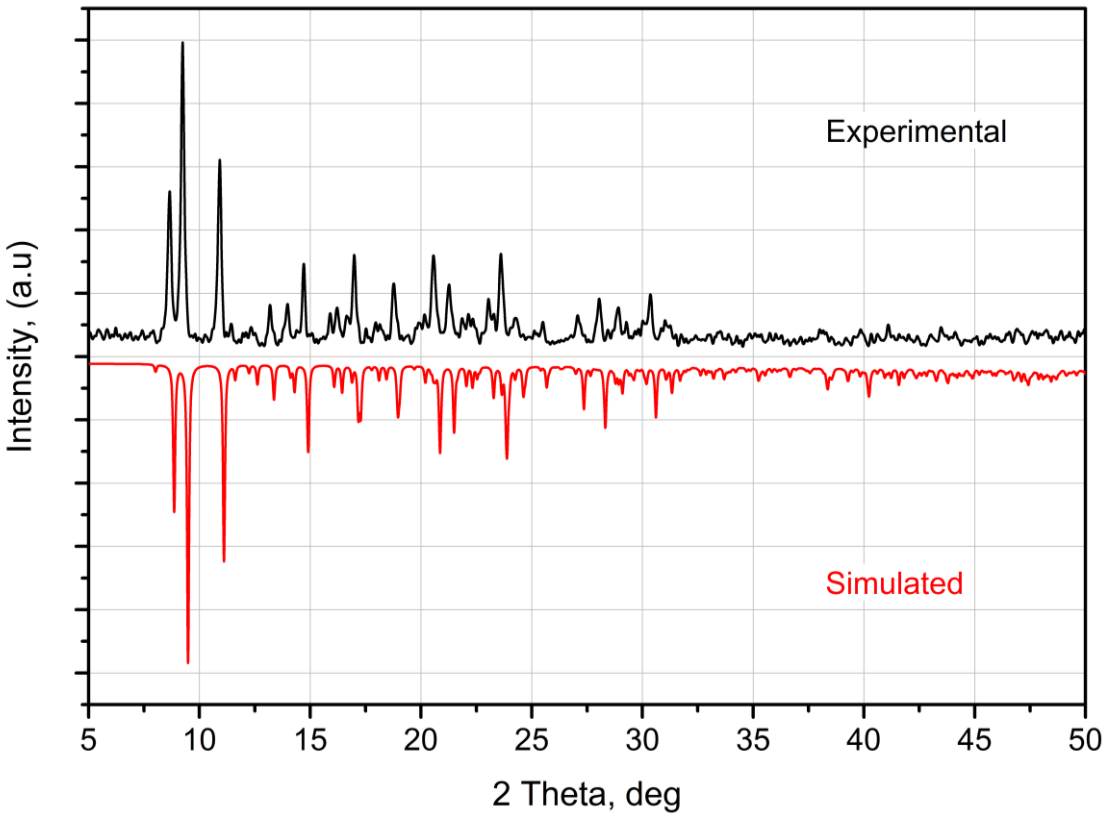

Figure S1. Comparison of the experimental PXRD pattern of as-synthesized **[Cu(Me$_3$pz)$_3${NbOF$_5$}]$_n$ (I)** with the simulated pattern calculated from SCXRD data.

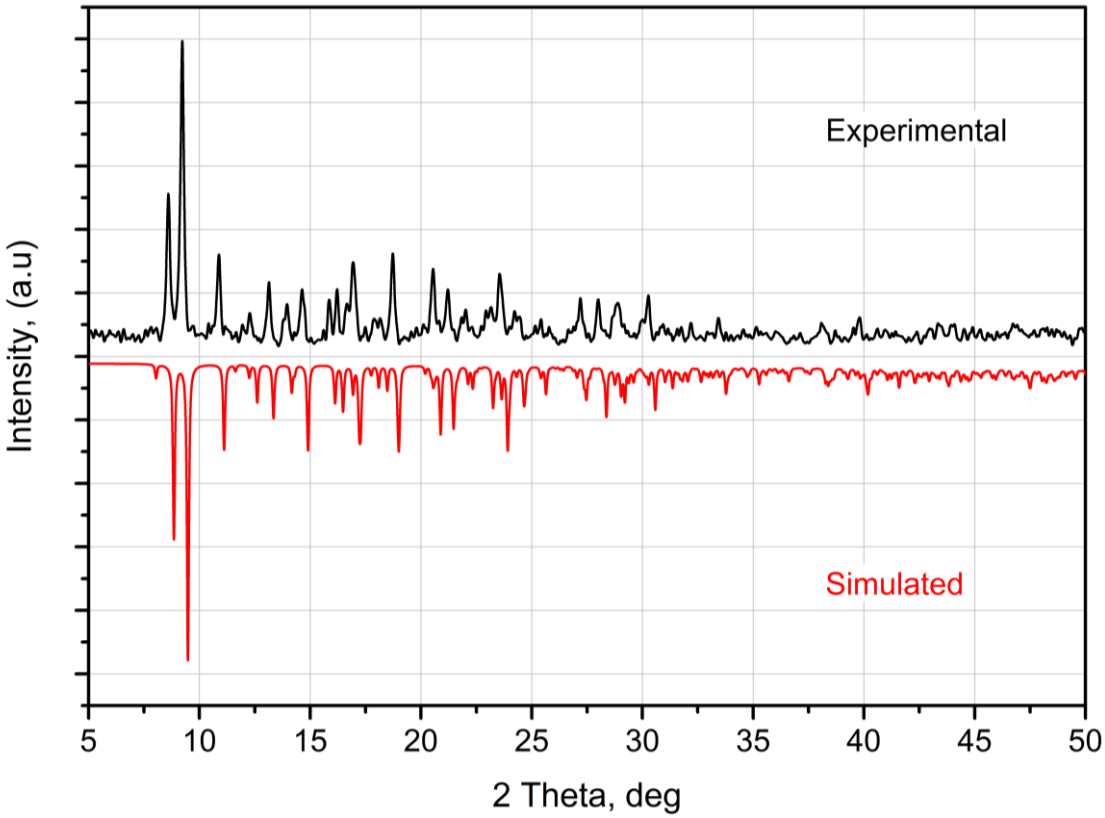

Figure S2. Comparison of the experimental PXRD pattern of as-synthesized **[Cu(Me$_3$pz)$_3${TaOF$_5$}]$_n$ (II)** with the simulated pattern calculated from SCXRD data.

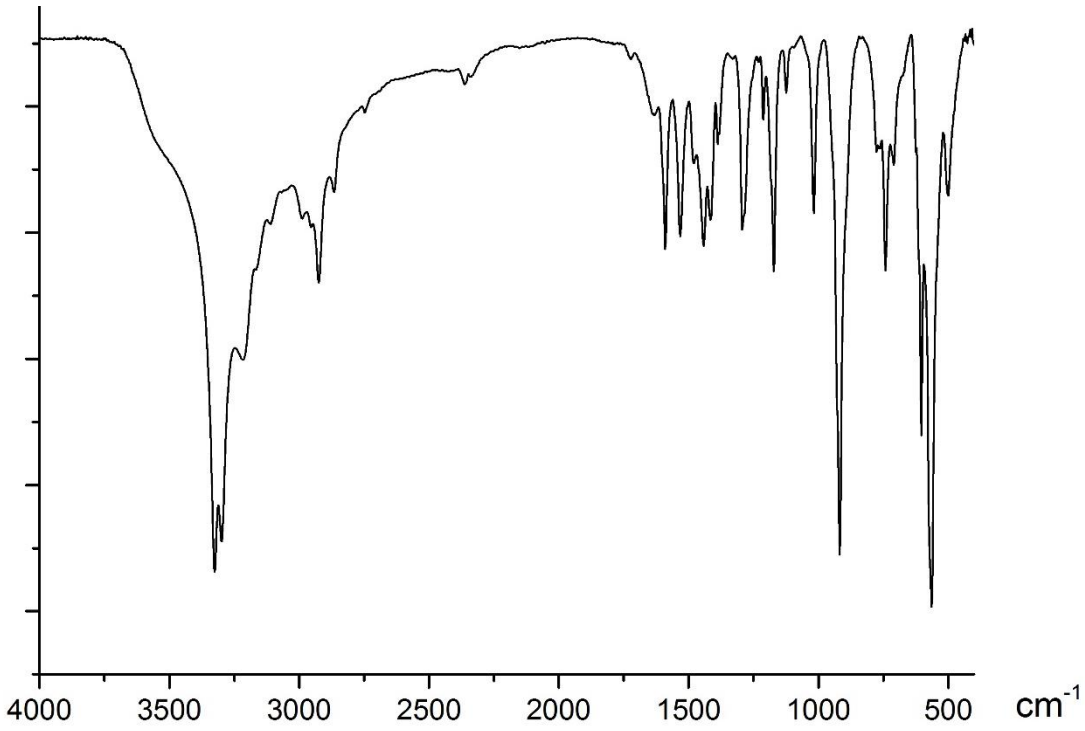

Figure S3. IR spectrum of **[Cu(Me$_3$pz)$_3${NbOF$_5$}]$_n$ (I)**: 500 m; 564 vs; 604 s; 710 w; 742 m; 776 w; 918 vs; 1018 m; 1124 w; 1172 m; 1212 w; 1294 m; 1388 w; 1416 m; 1442 m; 1480 w; 1532 m; 1590 m; 1632 w; 2866 w; 2924 m; 3218 s; 3298 vs; 3326 vs

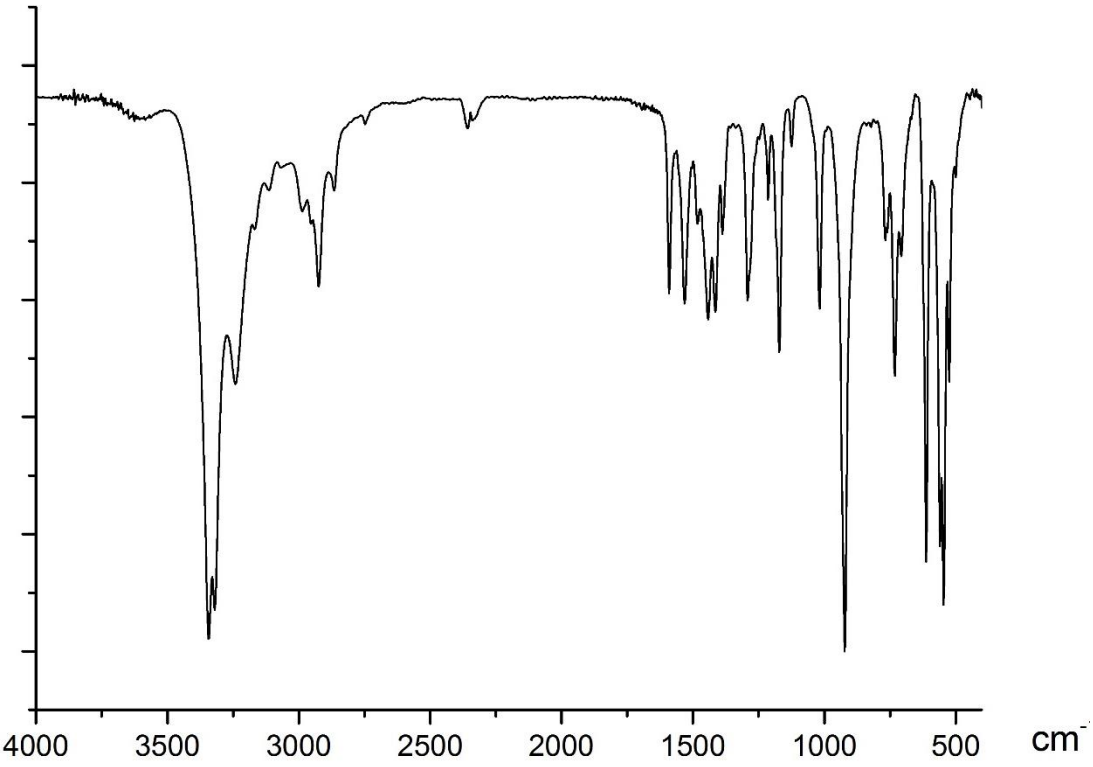

Figure S4. IR spectrum of **[Cu(Me$_3$pz)$_3${TaOF$_5$}]$_n$ (II)**: 500 w; 524 s; 546 vs; 560 vs; 612 vs; 708 m; 732 s; 768 m; 922 vs; 1018 m; 1124 w; 1172 m; 1214 w; 1292 m; 1388 w; 1414 m; 1442 m; 1482 w; 1532 m; 1590 m; 2866 w; 2924 m; 2986 w; 3114 w; 3242 s; 3320 vs; 3344 vs;

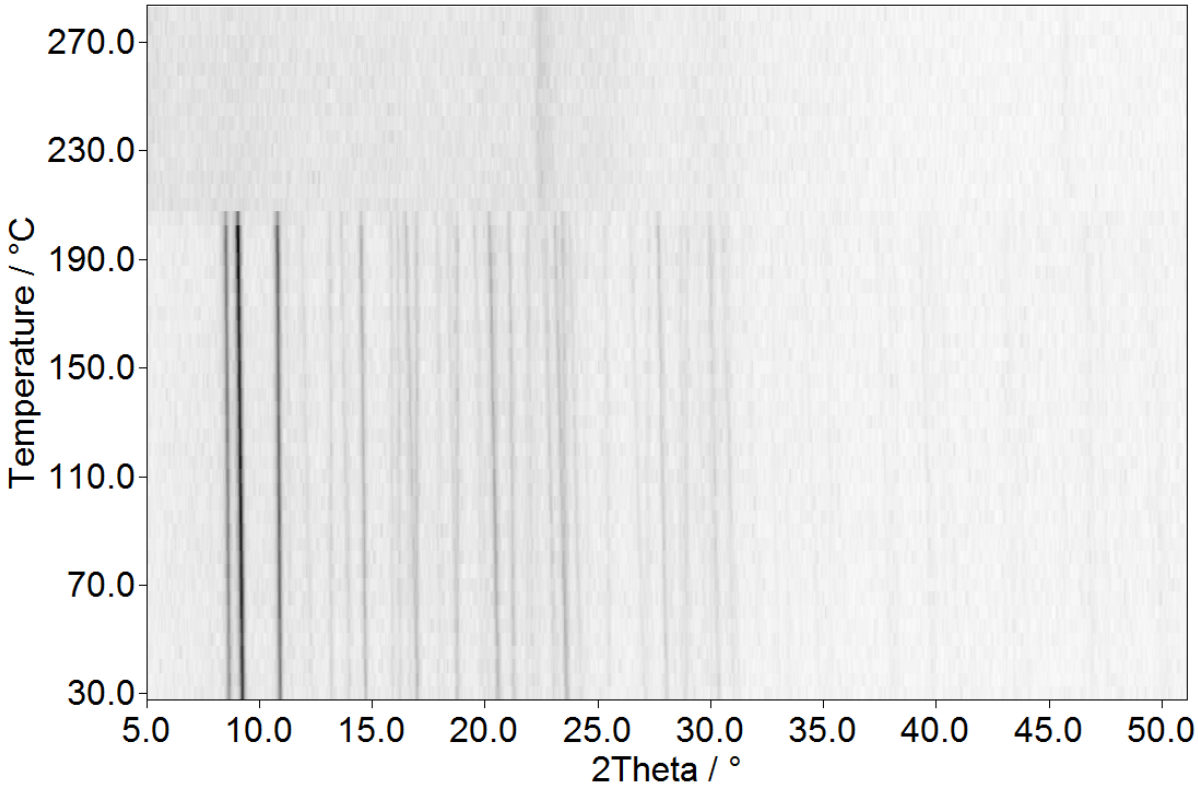

Figure S5. Thermo-PXRD pattern for **[Cu(Me$_3$pz)$_3${NbOF$_5$}]$_n$ (I)**

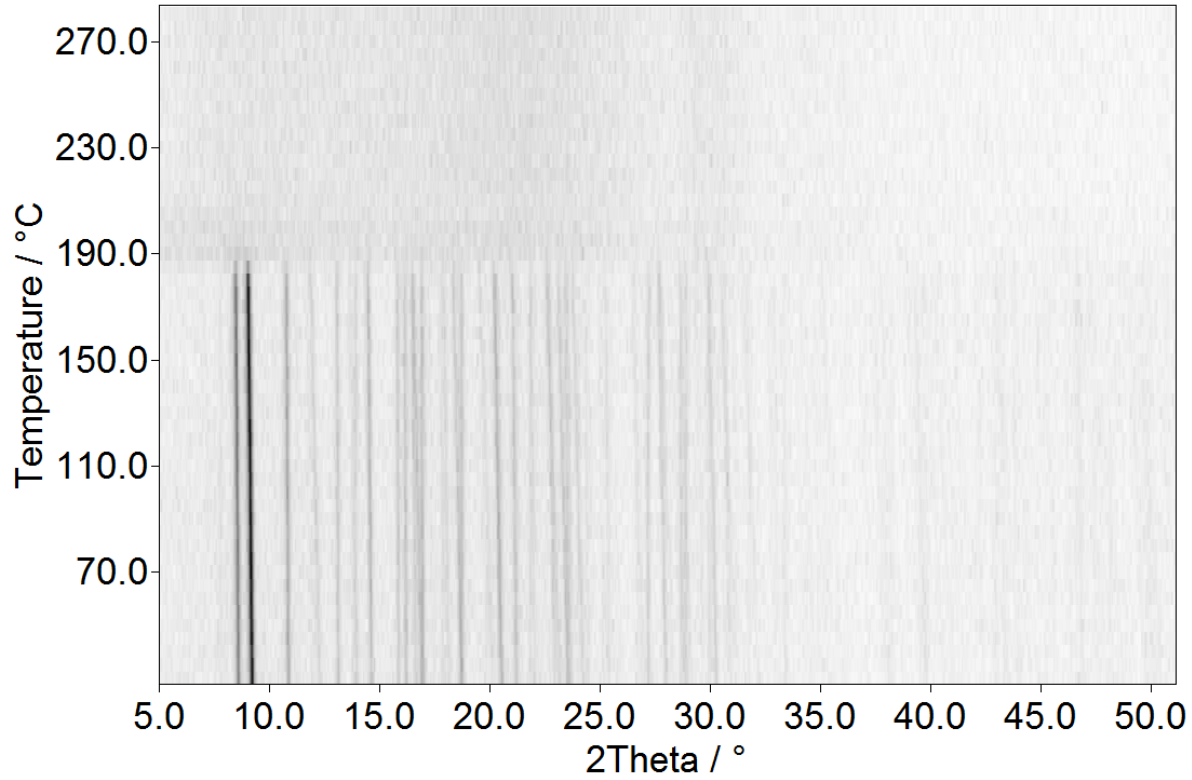

Figure S6. Thermo-PXRD pattern for **[Cu(Me$_3$pz)$_3${TaOF$_5$}]$_n$ (II)**

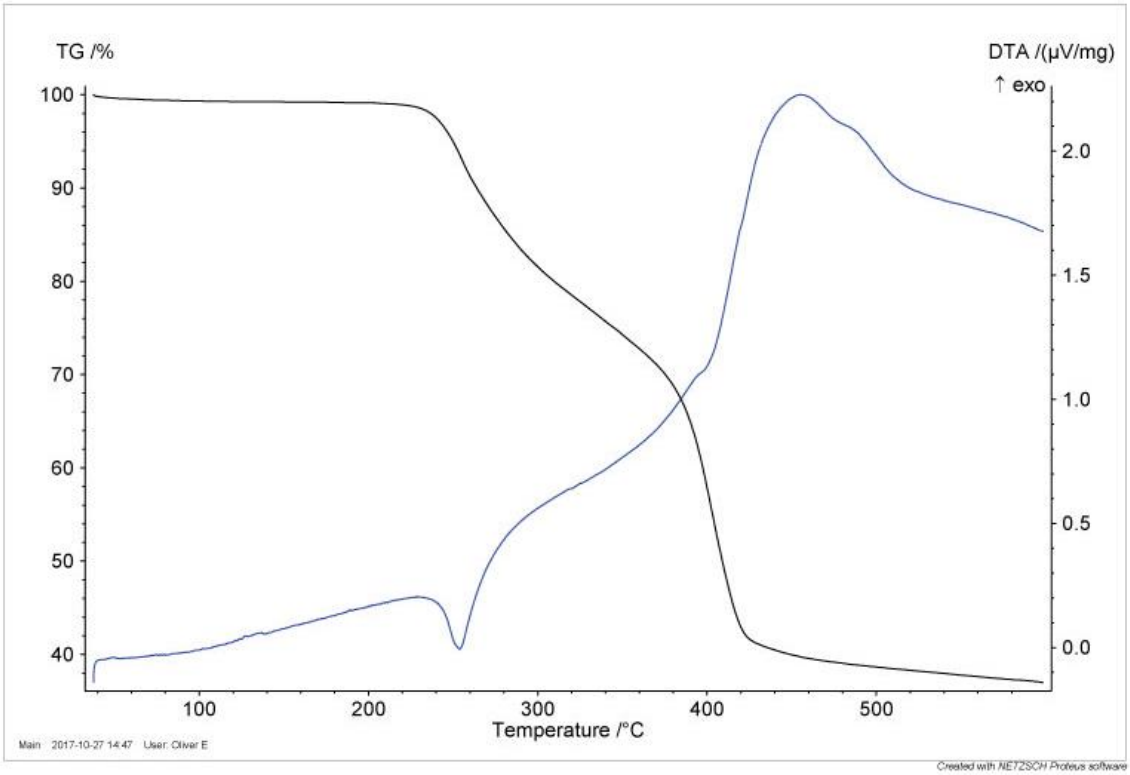

Figure S7. Thermoanalytical curves for **[Cu(Me$_3$pz)$_3${NbOF$_5$}]$_n$ (I)**

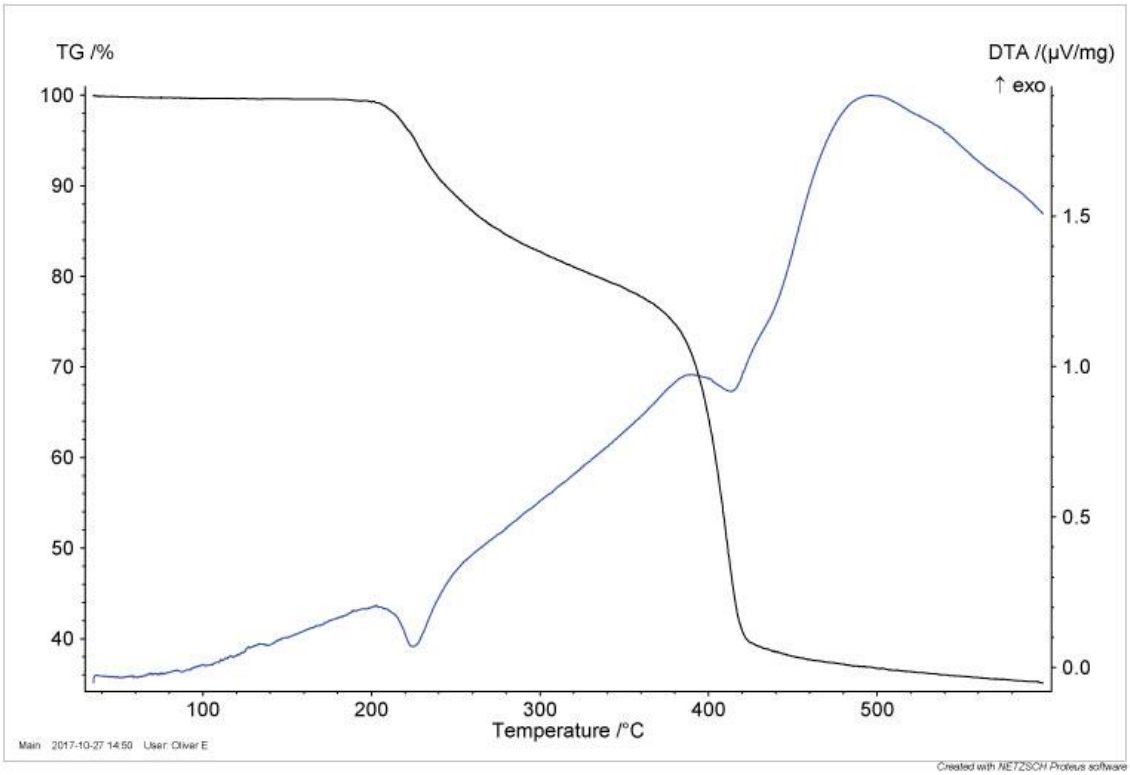

Figure S8. Thermoanalytical curves for **[Cu(Me$_3$pz)$_3${TaOF$_5$}]$_n$ (II)**